

G.E. Leblanc, et. al.. "Viscosity Measurement."

Copyright 2000 CRC Press LLC. <<http://www.engnetbase.com>>.

Viscosity Measurement

G.E. Leblanc

McMaster University

R.A. Secco

The University of Western Ontario

M. Kostic

Northern Illinois University

30.1 Shear Viscosity

Newtonian and Non-Newtonian Fluids • Dimensions and Units of Viscosity • Viscometer Types • Capillary Viscometers • Falling Body Methods • Oscillating Method • Ultrasonic Methods

30.1 Shear Viscosity

An important mechanical property of fluids is *viscosity*. Physical systems and applications as diverse as fluid flow in pipes, the flow of blood, lubrication of engine parts, the dynamics of raindrops, volcanic eruptions, planetary and stellar magnetic field generation, to name just a few, all involve fluid flow and are controlled to some degree by fluid viscosity. *Viscosity* is defined as the internal friction of a fluid. The microscopic nature of internal friction in a fluid is analogous to the macroscopic concept of mechanical friction in the system of an object moving on a stationary planar surface. Energy must be supplied (1) to overcome the inertial state of the interlocked object and plane caused by surface roughness, and (2) to initiate and sustain motion of the object over the plane. In a fluid, energy must be supplied (1) to create viscous flow units by breaking bonds between atoms and molecules, and (2) to cause the flow units to move relative to one another. The resistance of a fluid to the creation and motion of flow units is due to the viscosity of the fluid, which only manifests itself when motion in the fluid is set up. Since viscosity involves the transport of mass with a certain velocity, the viscous response is called a *momentum transport process*. The velocity of flow units within the fluid will vary, depending on location. Consider a liquid between two closely spaced parallel plates as shown in [Figure 30.1](#). A force, F , applied to the top plate causes the fluid adjacent to the upper plate to be dragged in the direction of F . The applied force is communicated to neighboring layers of fluid below, each coupled to the driving layer above, but with diminishing magnitude. This results in the progressive decrease in velocity of each fluid layer, as shown by the decreasing velocity vector in [Figure 30.1](#), away from the upper plate. In this system, the applied force is called a *shear* (when applied over an area it is called a *shear stress*), and the resulting deformation rate of the fluid, as illustrated by the *velocity gradient* dU_x/dz , is called the *shear strain rate*, $\dot{\gamma}_{zx}$. The mathematical expression describing the viscous response of the system to the shear stress is simply:

$$\tau_{zx} = \frac{\eta dU_x}{dz} = \eta \dot{\gamma}_{zx} \quad (30.1)$$

where τ_{zx} , the shear stress, is the force per unit area exerted on the upper plate in the x -direction (and hence is equal to the force per unit area exerted by the fluid on the upper plate in the x -direction under the assumption of a no-slip boundary layer at the fluid–upper plate interface); dU_x/dz is the gradient of the x -velocity in the z -direction in the fluid; and η is the *coefficient of viscosity*. In this case, because one is concerned with a shear force that produces the fluid motion, η is more specifically called the *shear*

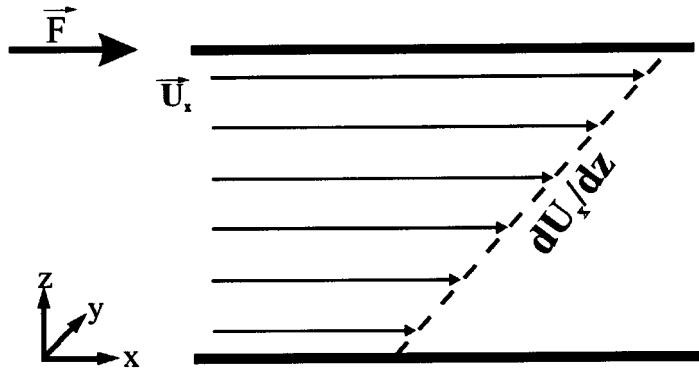


FIGURE 30.1 System for defining Newtonian viscosity. When the upper plate is subjected to a force, the fluid between the plates is dragged in the direction of the force with a velocity of each layer that diminishes away from the upper plate. The reducing velocity eventually reaches zero at the lower plate boundary.

dynamic viscosity. In fluid mechanics, diffusion of momentum is a more useful description of viscosity where the motion of a fluid is considered without reference to force. This type of viscosity is called the *kinematic viscosity*, ν , and is derived by dividing dynamic viscosity by ρ , the mass density:

$$\nu = \frac{\eta}{\rho} \quad (30.2)$$

The definition of viscosity by Equation 30.1 is valid only for *laminar* (i.e., layered or sheet-like) or streamline flow as depicted in Figure 30.1, and it refers to the molecular viscosity or *intrinsic viscosity*. The molecular viscosity is a property of the material that depends microscopically on bond strengths, and is characterized macroscopically as the fluid's resistance to flow. When the flow is turbulent, the diffusion of momentum is comprised of viscous contributions from the motion, sometimes called the *eddy viscosity*, in addition to the intrinsic viscosity. Viscosities of turbulent systems can be as high as 10^6 times greater than viscosities of laminar systems, depending on the Reynolds number.

Molecular viscosity is separated into *shear viscosity* and bulk or *volume viscosity*, η_v , depending on the type of strain involved. Shear viscosity is a measure of resistance to isochoric flow in a shear field, whereas volume viscosity is a measure of resistance to volumetric flow in a three-dimensional stress field. For most liquids, including hydrogen bonded, weakly associated or unassociated, and polymeric liquids as well as liquid metals, $\eta/\eta_v \approx 1$, suggesting that shear and structural viscous mechanisms are closely related [1].

The shear viscosity of most liquids decreases with temperature and increases with pressure, which is opposite to the corresponding responses for gases. An increase in temperature usually causes expansion and a corresponding reduction in liquid bond strength, which in turn reduces the internal friction. Pressure causes a decrease in volume and a corresponding increase in bond strength, which in turn enhances the internal friction. For most situations, including engineering applications, temperature effects dominate the antagonistic effects of pressure. However, in the context of planetary interiors where the effects of pressure cannot be ignored, pressure controls the viscosity to the extent that, depending on composition, it can cause fundamental changes in the molecular structure of the fluid that can result in an anomalous viscosity decrease with increasing pressure [2].

Newtonian and Non-Newtonian Fluids

Equation 30.1 is known as Newton's law of viscosity and it formulates Sir Isaac Newton's definition of the viscous behavior of a class of fluids now called Newtonian fluids.

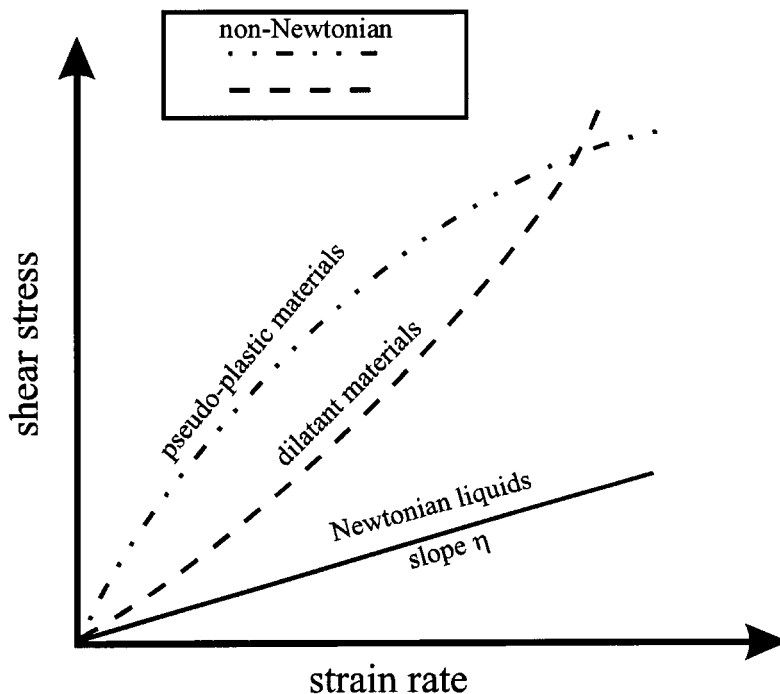


FIGURE 30.2 Flow curves illustrating Newtonian and non-Newtonian fluid behavior.

If the viscosity throughout the fluid is independent of strain rate, then the fluid is said to be a *Newtonian fluid*. The constant of proportionality is called the coefficient of viscosity, and a plot of stress vs. strain rate for Newtonian fluids yields a straight line with a slope of η , as shown by the solid line flow curve in Figure 30.2. Examples of Newtonian fluids are pure, single-phase, unassociated gases, liquids, and solutions of low molecular weight such as water. There is, however, a large group of fluids for which the viscosity is dependent on the strain rate. Such fluids are said to be non-Newtonian fluids and their study is called *rheology*. In differentiating between Newtonian and non-Newtonian behavior, it is helpful to consider the time scale (as well as the normal stress differences and phase shift in dynamic testing) involved in the process of a liquid responding to a shear perturbation. The velocity gradient, dU_x/dz , in the fluid is equal to the shear strain rate, $\dot{\gamma}$, and therefore the time scale related to the applied shear perturbation about the equilibrium state is t_s , where $t_s = \dot{\gamma}^{-1}$. A second time scale, t_r , called the *relaxation time*, characterizes the rate at which the relaxation of the strain in the fluid can be accomplished and is related to the time it takes for a typical flow unit to move a distance equivalent to its mean diameter. For Newtonian water, $t_r \sim 10^{-12}$ s and, because shear rates greater than 10^6 s $^{-1}$ are rare in practice, the time required for adjustment of the shear perturbation in water is much less than the shear perturbation period (i.e., $t_r \ll t_s$). However, for non-Newtonian macromolecular liquids like polymeric liquids, for colloidal and fiber suspensions, and for pastes and emulsions, the long response times of large viscous flow units can easily make $t_r > t_s$. An example of a non-Newtonian fluid is liquid elemental sulfur, in which long chains (polymers) of up to 100,000 sulfur atoms form flow units that are easily entangled, which bind the liquid in a “rigid-like” network. Another example of a well-known non-Newtonian fluid is tomato ketchup.

With reference to Figure 30.2, the more general form of Equation 30.1 also accounts for the nonlinear response. In terms of an initial shear stress required for flow to start, $\tau_{xy}(0)$, an initial linear term in the Newtonian limit of a small range of strain rate, $\dot{\gamma} \partial \tau_{xy}(0) / \partial \dot{\gamma}$, and a nonlinear term $O(\dot{\gamma}^2)$, the shear stress dependence on strain rate, $\tau_{xy}(\dot{\gamma})$ can be described as:

$$\tau_{xy}(\dot{\gamma}) = \tau_{xy}(0) + \frac{\dot{\gamma} \partial \tau_{xy}(0)}{\partial \dot{\gamma}} + O(\dot{\gamma}^2) \quad (30.3)$$

For a Newtonian fluid, the initial stress at zero shear rate is zero and the nonlinear function $O(\dot{\gamma}^2)$ is zero, so Equation 30.3 reduces to Equation 30.1, since $\partial \tau_{xy}(0)/\partial \dot{\gamma}$ then equals η . For a non-Newtonian fluid, $\tau_{xy}(0)$ may be zero but the nonlinear term $O(\dot{\gamma}^2)$ is nonzero. This characterizes fluids in which shear stress increases disproportionately with strain rate, as shown in the dashed-dotted flow curve in Figure 30.2, or decreases disproportionately with strain rate, as shown in the dashed flow curve in Figure 30.2. The former type of fluid behavior is known as *shear thickening* or dilatancy, and an example is a concentrated solution of sugar in water. The latter, much more common type of fluid behavior, is known as *shear thinning* or pseudo-plasticity; cream, blood, most polymers, and liquid cement are all examples. Both behaviors result from particle or molecular reorientations in the fluid that increase or decrease, respectively, the internal friction to shear. Non-Newtonian behavior can also arise in fluids whose viscosity changes with time of applied shear stress. The viscosity of corn starch and water increases with time duration of stress, and this is called *rheopectic behavior*. Conversely, liquids whose viscosity decreases with time, like nondrip paints, which behave like solids until the stress applied by the paint brush for a sufficiently long time causes them to flow freely, are called *thixotropic fluids*.

Fluid deformation that is not recoverable after removal of the stress is typical of the purely viscous response. The other extreme response to an external stress is purely elastic and is characterized by an equilibrium deformation that is fully recovered on removal of the stress. There are an infinite number of intermediate or combined viscous/elastic responses to external stress, which are grouped under the behavior known as *viscoelasticity*. Fluids that behave elastically in some stress range require a limiting or yield stress before they will flow as a viscous fluid. A simple, empirical, constitutive equation often used for this type of rheological behavior is of the form:

$$\tau_{yx} = \tau_y + \dot{\gamma}^n \eta_p \quad (30.4)$$

where τ_y is the *yield stress*, η_p is an *apparent viscosity* called the plastic viscosity, and the exponent n allows for a range of non-Newtonian responses: $n = 1$ is pseudo-Newtonian behavior and is called a *Bingham fluid*; $n < 1$ is shear thinning behavior; and $n > 1$ is shear thickening behavior. Interested readers should consult [3–9] for further information on applied rheology.

Dimensions and Units of Viscosity

From Equation 30.1, the dimensions of dynamic viscosity are $M L^{-1} T^{-1}$ and the basic SI unit is the Pascal second (Pa·s), where $1 \text{ Pa}\cdot\text{s} = 1 \text{ N s m}^{-2}$. The c.g.s. unit of dyn s cm^{-2} is the poise (P). The dimensions of kinematic viscosity, from Equation 30.2, are $L^2 T^{-1}$ and the SI unit is $\text{m}^2 \text{ s}^{-1}$. For most practical situations, this is usually too large and so the c.g.s. unit of $\text{cm}^2 \text{ s}^{-1}$, or the stoke (St), is preferred. Table 30.1 lists some common fluids and their shear dynamic viscosities at atmospheric pressure and 20°C.

TABLE 30.1 Shear Dynamic Viscosity of Some Common Fluids at 20°C and 1 atm

Fluid	Shear dynamic viscosity (Pa·s)
Air	1.8×10^{-4}
Water	1.0×10^{-3}
Mercury	1.6×10^{-3}
Automotive engine oil (SAE 10W30)	1.3×10^{-1}
Dish soap	4.0×10^{-1}
Corn syrup	6.0

TABLE 30.2 Viscometer Classification and Basic Characteristics

Drag Flow Types:

Flow set by motion of instrument boundary/surface using external or gravity force.

Type/Geometry	Basic characteristics/Comments
Rotating concentric cylinders (Couette)	Good for low viscosity, high shear rates; for $R_2/R_1 \cong 1$, see Figure 30.3; hard to clean thick fluids
Rotating cone and plate	Homogeneous shear, best for non-Newtonian fluids and normal stresses; need good alignment, problems with loading and evaporation
Rotating parallel disks	Similar to cone-and-plate, but inhomogeneous shear; shear varies with gap height, easy sample loading
Sliding parallel plates	Homogeneous shear, simple design, good for high viscosity; difficult loading and gap control
Falling body (ball, cylinder)	Very simple, good for high temperature and pressure; need density and special sensors for opaque fluids, not good for viscoelastic fluids
Rising bubble	Similar to falling body viscometer; for transparent fluids
Oscillating body	Needs instrument constant, good for low viscous liquid metals

Pressure Flow Types:

Fluid set in motion in fixed instrument geometry by external or gravity pressure

Type/Geometry	Basic characteristics/Comments
Long capillary (Poiseuille flow)	Simple, very high shears and range, but very inhomogeneous shear, bad for time dependency, and is time consuming
Orifice/Cup (short capillary)	Very simple, reliable, but not for absolute viscosity and non-Newtonian fluids
Slit (parallel plates) pressure flow	Similar to capillary, but difficult to clean
Axial annulus pressure flow	Similar to capillary, better shear uniformity, but more complex, eccentricity problem and difficult to clean

Others/Miscellaneous:

Type/geometry	Basic characteristics/Comments
Ultrasonic	Good for high viscosity fluids, small sample volume, gives shear and volume viscosity, and elastic property data; problems with surface finish and alignment, complicated data reduction

Adapted from C. W. Macosko, *Rheology: Principles, Measurements, and Applications*, New York: VCH, 1994.

Viscometer Types

The instruments for viscosity measurements are designed to determine “a fluid’s resistance to flow,” a fluid property defined above as viscosity. The fluid flow in a given instrument geometry defines the strain rates, and the corresponding stresses are the measure of resistance to flow. If strain rate or stress is set and controlled, then the other one will, everything else being the same, depend on the fluid viscosity. If the flow is simple (one dimensional, if possible) such that the strain rate and stress can be determined accurately from the measured quantities, the absolute dynamic viscosity can be determined; otherwise, the relative viscosity will be established. For example, the fluid flow can be set by dragging fluid with a sliding or rotating surface, falling body through the fluid, or by forcing the fluid (by external pressure or gravity) to flow through a fixed geometry, such as a capillary tube, annulus, a slit (between two parallel plates), or orifice. The corresponding resistance to flow is measured as the boundary force or torque, or pressure drop. The flow rate or efflux time represents the fluid flow for a set flow resistance, like pressure drop or gravity force. The viscometers are classified, depending on how the flow is initiated or maintained, as in [Table 30.2](#).

The basic principle of all viscometers is to provide as simple flow kinematics as possible, preferably one-dimensional (*isometric*) flow, in order to determine the shear strain rate accurately, easily, and independent of fluid type. The resistance to such flow is measured, and thereby the shearing stress is

TABLE 30.3 Different Causes of Viscometers Errors

Error/Effect	Cause/Comment
End/edge effect	Energy losses at the fluid entrance and exit of main test geometry
Kinetic energy losses	Loss of pressure to kinetic energy
Secondary flow	Energy loss due to unwanted secondary flow, vortices, etc.; increases with Reynolds number
Nonideal geometry	Deviations from ideal shape, alignment, and finish
Shear rate non-uniformity	Important for non-Newtonian fluids
Temperature variation and viscous heating	Variation in temperature, in time and space, influences the measured viscosity
Turbulence	Partial and/or local turbulence often develops even at low Reynolds numbers
Surface tension	Difference in interfacial tensions
Elastic effects	Structural and fluid elastic effects
Miscellaneous effects	Depends on test specimen, melt fracture, thixotropy, rheopexy

TABLE 30.4 Viscometer Manufacturers

Manufacturers	Model	Description
Brookfield Eng. Labs Inc.	DV-I+	Concentric cylinder
Custom Scientific Inst. Inc.	CS245	Concentric cylinder
Reologica Inst.	Various	Falling sphere, capillary, rotational
Haake GmbH	Various	Falling sphere, rotational
Cannon Inst. Co.	Various	Extensive variety of capillary viscometers
Toyo Seiki Seisaku-Sho Ltd.	Capirograph	Capillary
Gottfert Werkstoff-Prufmaschinen GmbH	Various	Extensive variety of capillary viscometers
Cole-Palmer Inst. Co.	GV2100	Falling sphere
Paar Physica U.S.A. Inc.	Various	Concentric cylinder, falling sphere, capillary
Monsanto Inst. & Equipment	ODR 2000	Oscillating viscometer
Nametree Co.	Vibrational viscometer	Oscillating viscometer
Rheometric Scientific Inc.	RM180	Cone-and-plate, parallel plate
	RM265	Concentric cylinders
T.A. Instruments Inc.	Various	Concentric cylinder

Note: All the above manufacturers can be found via the Internet (World Wide Web), along with the most recent contact information, product description and in some cases, pricing.

determined. The shear viscosity is then easily found as the ratio between the shearing stress and the corresponding shear strain rate. Practically, it is never possible to achieve desired one-dimensional flow nor ideal geometry, and a number of errors, listed in [Table 30.3](#), can occur and need to be accounted for [4–8]. A list of manufacturers/distributors of commercial viscometers/rheometers is given in [Table 30.4](#).

Concentric Cylinders

The main advantage of the rotational as compared to many other viscometers is its ability to operate continuously at a given shear rate, so that other steady-state measurements can be conveniently performed. That way, time dependency, if any, can be detected and determined. Also, subsequent measurements can be made with the same instrument and sampled at different shear rates, temperature, etc. For these and other reasons, *rotational viscometers* are among the most widely used class of instruments for rheological measurements.

Concentric cylinder-type viscometers/rheometers are usually employed when absolute viscosity needs to be determined, which in turn, requires a knowledge of well-defined shear rate and shear stress data. Such instruments are available in different configurations and can be used for almost any fluid. There are models for low and high shear rates. More complete discussion on concentric cylinder viscometers/rheometers is given elsewhere [4–9]. In the *Couette-type viscometer*, the rotation of the outer cylinder, or cup, minimizes centrifugal forces, which cause Taylor vortices. The latter can be present in the *Searle-type viscometer* when the inner cylinder, or bob, rotates.

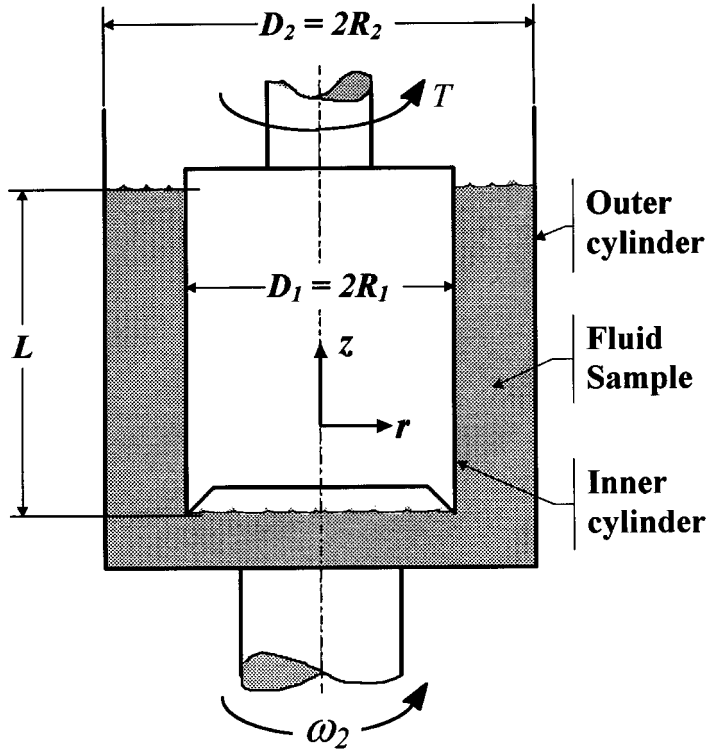


FIGURE 30.3 Concentric cylinders viscometer geometry.

Usually, the torque on the stationary cylinder and rotational velocity of the other cylinder are measured for determination of the shear stress and shear rate, which is needed for viscosity calculation. Once the torque, T , is measured, it is simple to describe the fluid shear stress at any point with radius r between the two cylinders, as shown in Figure 30.3.

$$\tau_{r\theta}(r) = \frac{T}{2\pi r^2 L_e} \quad (30.5)$$

In Equation 30.5, $L_e = (L + L_e)$, is the effective length of the cylinder at which the torque is measured. In addition to the cylinder's length L , it takes into account the end-effect correction L_e [4–8].

For a narrow gap between the cylinders ($\beta = R_2/R_1 \cong 1$), regardless of the fluid type, the velocity profile can be approximated as linear, and the shear rate within the gap will be uniform:

$$\gamma(r) \cong \frac{\Omega \bar{R}}{(R_2 - R_1)} \quad (30.6)$$

where $\Omega = (\omega_2 - \omega_1)$ is the relative rotational speed and $\bar{R} = (R_1 + R_2)/2$, is the mean radius of the inner (1) and outer (2) cylinders. Actually, the shear rate profile across the gap between the cylinders depends on the relative rotational speed, radii, and the unknown fluid properties, which seems an “open-ended” enigma. The solution of this complex problem is given elsewhere [4–8] in the form of an infinite series, and requires the slope of a logarithmic plot of T as a function of Ω in the range of interest. Note that for a stationary inner cylinder ($\omega_1 = 0$), which is the usual case in practice, Ω becomes equal to ω_2 .

However, there is a simpler procedure [10] that has also been established by German standards [11]. For any fluid, including non-Newtonian fluids, there is a radius at which the shear rate is virtually independent of the fluid type for a given Ω . This radius, being a function of geometry only, is called the *representative radius*, R_R , and is determined as the location corresponding to the so-called representative shear stress, $\tau_R = (\tau_1 + \tau_2)/2$, the average of the stresses at the outer and inner cylinder interfaces with the fluid, that is:

$$R_R = R_1 \left\{ \frac{[2\beta^2]}{[1+\beta^2]} \right\}^{1/2} = R_2 \left\{ \frac{2}{[1+\beta^2]} \right\}^{1/2} \quad (30.7)$$

Since the shear rate at the representative radius is virtually independent on the fluid type (whether Newtonian or non-Newtonian), the representative shear rate is simply calculated for Newtonian fluid ($n = 1$) and $r = R_R$, according to [10]:

$$\dot{\gamma}_R = \dot{\gamma}_{r=R_R} = \omega_2 \left\{ \frac{[\beta^2 + 1]}{[\beta^2 - 1]} \right\} \quad (30.8)$$

The accuracy of the representative parameters depends on the geometry of the cylinders (β) and fluid type (n).

It is shown in [10] that, for an unrealistically wide range of fluid types ($0.35 < n < 3.5$) and cylinder geometries ($\beta = 1$ to 1.2), the maximum errors are less than 1%. Therefore, the error associated with the representative parameters concept is virtually negligible for practical measurements.

Finally, the (apparent) fluid viscosity is determined as the ratio between the shear stress and corresponding shear rate using Equations 30.5 to 30.8, as:

$$\eta = \eta_R = \frac{\tau_R}{\dot{\gamma}_R} = \left\{ \frac{[\beta^2 - 1]}{[4\pi\beta^2 R_1^2 L_c]} \right\} \frac{T}{\omega_2} = \left\{ \frac{[\beta^2 - 1]}{[4\pi R_2^2 L_c]} \right\} \frac{T}{\omega_2} \quad (30.9)$$

For a given cylinder geometry (β , R_2 , and L_c), the viscosity can be determined from Equation 30.8 by measuring T and ω_2 .

As already mentioned, in Couette-type viscometers, the Taylor vortices within the gap are virtually eliminated. However, vortices at the bottom can be present, and their influence becomes important when the Reynolds number reaches the value of unity [10, 11]. Furthermore, flow instability and turbulence will develop when the Reynolds number reaches values of 10^3 to 10^4 . The Reynolds number, Re , for the flow between concentric cylinders is defined [11] as:

$$Re = \left\{ \frac{[\rho\omega_2 R_1^2]}{2\eta} \right\} [\beta^2 - 1] \quad (30.10)$$

Cone-and-Plate Viscometers

The simple cone-and-plate viscometer geometry provides a uniform rate of shear and direct measurements of the first normal stress difference. It is the most popular instrument for measurement of non-Newtonian fluid properties. The working shear stress and shear strain rate equations can be easily derived in spherical coordinates, as indicated by the geometry in [Figure 30.4](#), and are, respectively:

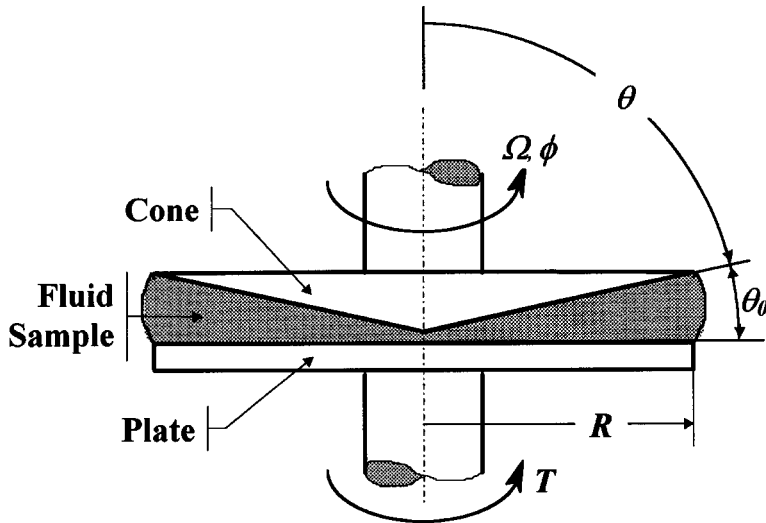


FIGURE 30.4 Cone-and-plate viscometer geometry.

$$\tau_{\theta\phi} = \frac{3T}{2\pi R^3} \quad (30.11)$$

and

$$\dot{\gamma} = \frac{\Omega}{\theta_0} \quad (30.12)$$

where R and $\theta_0 < 0.1$ rad ($\approx 6^\circ$) are the cone radius and angle, respectively. The viscosity is then easily calculated as:

$$\eta = \frac{\tau_{\theta\phi}}{\dot{\gamma}} = \frac{3T\theta_0}{2\pi\Omega R^3} \quad (30.13)$$

Inertia and secondary flow increase while shear heating decreases the measured torque (T_m). For more details, see [4, 5]. The torque correction is given as:

$$\frac{T_m}{T} = 1 + 6 \cdot 10^{-4} \text{Re}^2 \quad (30.14)$$

where

$$\text{Re} = \frac{\left\{ \rho [\Omega \theta_0 R]^2 \right\}}{\eta} \quad (30.15)$$

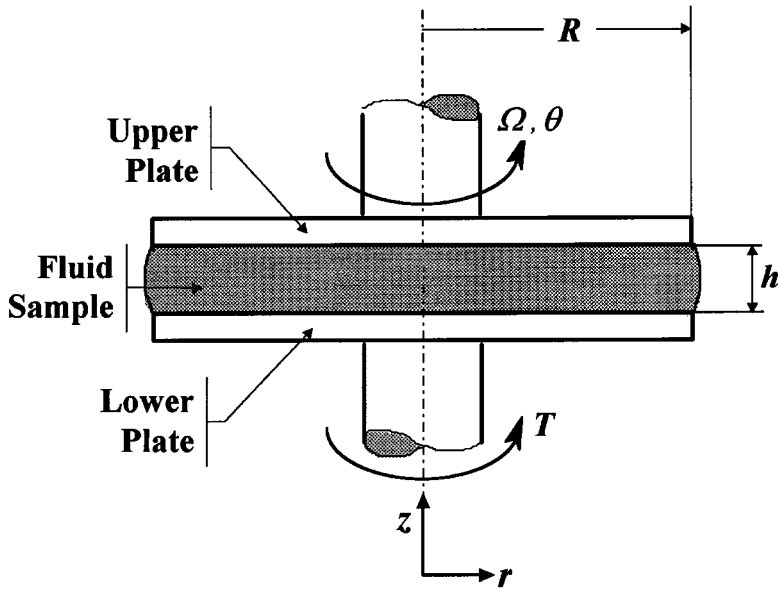


FIGURE 30.5 Parallel disks viscometer geometry.

Parallel Disks

This geometry (Figure 30.5), which consists of a disk rotating in a cylindrical cavity, is similar to the cone-and-plate geometry, and many instruments permit the use of either one. However, the shear rate is no longer uniform, but depends on radial distance from the axis of rotation and on the gap h , that is:

$$\dot{\gamma}(r) = \frac{r\Omega}{h} \quad (30.16)$$

For Newtonian fluids, after integration over the disk area, the torque can be expressed as a function of viscosity, so that the latter can be determined as:

$$\eta = \frac{2Th}{\pi\Omega R^4} \quad (30.17)$$

Capillary Viscometers

The *capillary viscometer* is based on the fully developed laminar tube flow theory (*Hagen–Poiseuille flow*) and is shown in Figure 30.6. The capillary tube length is many times larger than its small diameter, so that entrance flow is neglected or accounted for in more accurate measurement or for shorter tubes. The expression for the shear stress at the wall is:

$$\tau_w = \left[\frac{\Delta P}{L} \right] \cdot \left[\frac{D}{4} \right] \quad (30.18)$$

and

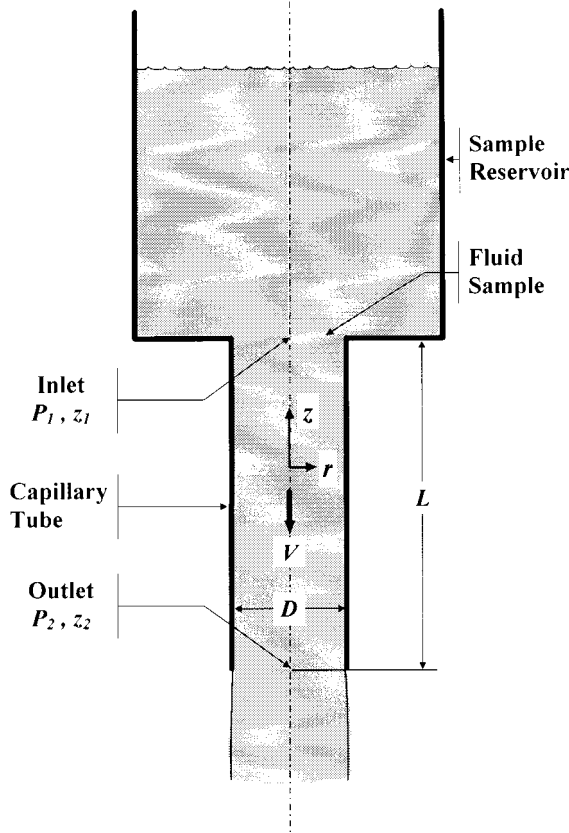


FIGURE 30.6 Capillary viscometer geometry.

$$\Delta P = (P_1 - P_2) + (z_1 - z_2) - \frac{[C_p V^2]}{2} \quad (30.19)$$

where, $C \cong 1.1$, B , z , $V = 4Q/[\pi D^2]$, and Q are correction factor, pressure, elevation, the mean flow velocity, and the fluid volume-flow rate, respectively. The subscripts 1 and 2 refer to the inlet and outlet, respectively.

The expression for the shear rate at the wall is:

$$\dot{\gamma} = \left\{ \frac{[3n+1]}{4n} \right\} \circ \left\{ \frac{8V}{D} \right\} \quad (30.20)$$

where $n = d[\log \tau_w]/d[\log (8V/D)]$ is the slope of the measured $\log(\tau_w) - \log (8V/D)$ curve. Then, the viscosity is simply calculated as:

$$\eta = \frac{\tau_w}{\dot{\gamma}} = \left\{ \frac{4n}{[3n+1]} \right\} \circ \left\{ \frac{\Delta P D^2}{[32LV]} \right\} = \left\{ \frac{4n}{[3n+1]} \right\} \circ \left\{ \frac{[\Delta P D^4 \pi]}{[128QL]} \right\} \quad (30.21)$$

Note that $n = 1$ for a Newtonian fluid, so the first term, $[4n/(3n + 1)]$ becomes unity and disappears from the above equations. The advantages of capillary over rotational viscometers are low cost, high accuracy (particularly with longer tubes), and the ability to achieve very high shear rates, even with high-viscosity samples. The main disadvantages are high residence time and variation of shear across the flow, which can change the structure of complex test fluids, as well as shear heating with high-viscosity samples.

Glass Capillary Viscometers

Glass capillary viscometers are very simple and inexpensive. Their geometry resembles a U-tube with at least two reservoir bulbs connected to a capillary tube passage with inner diameter D . The fluid is drawn up into one bulb reservoir of known volume, V_0 , between etched marks. The efflux time, Δt , is measured for that volume to flow through the capillary under gravity.

From Equation 30.21 and taking into account that $V_0 = (\Delta t)VD^2\pi/4$ and $\Delta P = \rho g(z_1 - z_2)$, the kinematic viscosity can be expressed as a function of the efflux time only, with the last term, $K/\Delta t$, added to account for error correction, where K is a constant [7]:

$$v = \frac{\eta}{\rho} = \left\{ \left[\frac{4n}{(3n+1)} \right] \cdot \frac{[\pi g(z_1 - z_2)D^4]}{128LV_0} \right\} (\Delta t - K\Delta t) \quad (30.22)$$

Note that for a given capillary viscometer and $n \cong 1$, the bracketed term is a constant. The last correction term is negligible for a large capillary tube ratio, L/D , where kinematic viscosity becomes linearly proportional to measured efflux time. Various kinds of commercial glass capillary viscometers, like Cannon–Fenske type or similar, can be purchased from scientific and/or supply stores. They are the modified original *Ostwald viscometer* design in order to minimize certain undesirable effects, to increase the viscosity range, or to meet specific requirements of the tested fluids, like opacity, etc. Glass capillary viscometers are often used for low-viscosity fluids.

Orifice/Cup, Short Capillary: Saybolt Viscometer

The principle of these viscometers is similar to glass capillary viscometers, except that the flow through a short capillary ($L/D \ll 10$) does not satisfy or even approximate the Hagen–Poiseuille, fully developed, pipe flow. The influences of entrance end-effect and changing hydrostatic heads are considerable. The efflux time reading, Δt , represents relative viscosity for comparison purposes and is expressed as “viscometer seconds,” like the Saybolt seconds, or Engler seconds or degrees. Although the conversion formula, similar to glass capillary viscometers, is used, the constants k and K in Equation 30.23 are purely empirical and dependent on fluid types.

$$v = \frac{\eta}{\rho} = k\Delta t - \frac{K}{\Delta t} \quad (30.23)$$

where $k = 0.00226, 0.0216, 0.073$; and $K = 1.95, 0.60, 0.0631$; for Saybolt Universal ($\Delta t < 100$ s), Saybolt Furol ($\Delta t > 40$ s), and Engler viscometers, respectively [12, 13]. Due to their simplicity, reliability, and low cost, these viscometers are widely used for Newtonian fluids, like in oil and other industries, where the simple correlations between the relative properties and desired results are needed. However, these viscometers are not suitable for absolute viscosity measurement, nor for non-Newtonian fluids.

Falling Body Methods

Falling Sphere

The falling sphere viscometer is one of the earliest and least involved methods to determine the absolute shear viscosity of a Newtonian fluid. In this method, a sphere is allowed to fall freely a measured distance

through a viscous liquid medium and its velocity is determined. The viscous drag of the falling sphere results in the creation of a restraining force, F , described by Stokes' law:

$$F = 6\pi\eta r_s U_t \quad (30.24)$$

where r_s is the radius of the sphere and U_t is the *terminal velocity* of the falling body. If a sphere of density ρ_2 is falling through a fluid of density ρ_1 in a container of infinite extent, then by balancing Equation 30.24 with the net force of gravity and buoyancy exerted on a solid sphere, the resulting equation of absolute viscosity is:

$$\eta = 2gr_s^2 \frac{(\rho_2 - \rho_1)}{9U_t} \quad (30.25)$$

Equation 30.25 shows the relation between the viscosity of a fluid and the terminal velocity of a sphere falling within it. Having a finite container volume necessitates the modification of Equation 30.25 to correct for effects on the velocity of the sphere due to its interaction with container walls (W) and ends (E). Considering a cylindrical container of radius r and height H , the corrected form of Equation 30.25 can be written as:

$$\eta = 2gr_s^2 \frac{(\rho_2 - \rho_1)W}{(9U_t E)} \quad (30.26)$$

where

$$W = 1 - 2.104 \left(\frac{r_s}{r} \right) + 2.09 \left(\frac{r_s}{r} \right)^3 - 0.95 \left(\frac{r_s}{r} \right)^5 \quad (30.27)$$

$$E = 1 + 3.3 \left(\frac{r_s}{H} \right) \quad (30.28)$$

The wall correction was empirically derived [15] and is valid for $0.16 \leq r_s/r \leq 0.32$. Beyond this range, the effects of container walls significantly impair the terminal velocity of the sphere, thus giving rise to a false high viscosity value.

Figure 30.7 is a schematic diagram of the falling sphere method and demonstrates the attraction of this method — its simplicity of design. The simplest and most cost-effective approach in applying this method to transparent liquids would be to use a sufficiently large graduated cylinder filled with the liquid. With a distance marked on the cylinder near the axial and radial center (the region least influenced by the container walls and ends), a sphere (such as a ball bearing or a material that is nonreactive with the liquid) with a known density and sized to within the bounds of the container correction, free falls the length of the cylinder. As the sphere passes through the marked region of length d at its terminal velocity, a measure of the time taken to traverse this distance allows the velocity of the sphere to be calculated. Having measured all the parameters of Equation 30.26, the shear viscosity of the liquid can be determined.

This method is useful for liquids with viscosities between 10^{-3} Pa·s and 10^5 Pa·s. Due to the simplicity of design, the falling sphere method is particularly well suited to high pressure–high temperature viscosity studies.

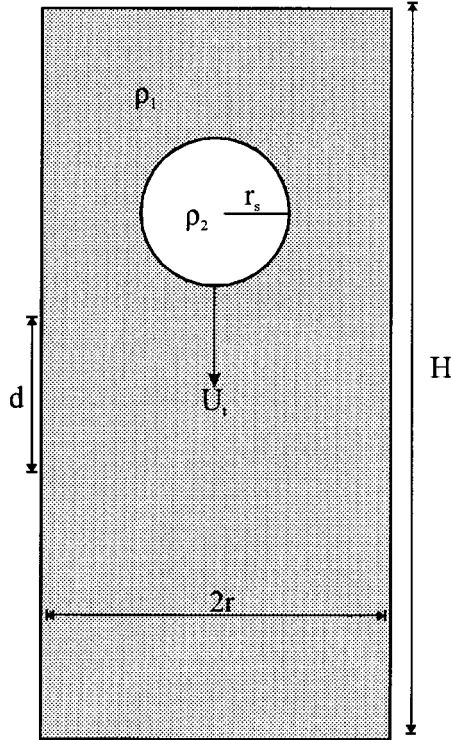


FIGURE 30.7 Schematic diagram of the falling sphere viscometer. Visual observations of the time taken for the sphere to traverse the distance d , is used to determine a velocity of the sphere. The calculated velocity is then used in Equation 30.24 to determine a shear viscosity.

Falling Cylinder

The *falling cylinder method* is similar in concept to the falling sphere method except that a flat-ended, solid circular cylinder freely falls vertically in the direction of its longitudinal axis through a liquid sample within a cylindrical container. A schematic diagram of the configuration is shown in Figure 30.8. Taking an infinitely long cylinder of density ρ_2 and radius r_c falling through a Newtonian fluid of density ρ_1 with infinite extent, the resulting shear viscosity of the fluid is given as:

$$\eta = gr_c^2 \frac{(\rho_2 - \rho_1)}{2U_t} \quad (30.29)$$

Just as with the falling sphere, a finite container volume necessitates modifying Equation 30.29 to account for the effects of container walls and ends. A correction for container wall effects can be analytically deduced by balancing the buoyancy and gravitational forces on the cylinder, of length L , with the shear force on the sides and the compressional force on the cylinder's leading end and the tensile force on the cylinder's trailing end. The resulting correction term, or geometrical factor, $G(k)$ (where $k = r_c/r$), depends on the cylinder radius and the container radius, r , and is given by:

$$G(k) = \frac{[k^2(1 - \ln k) - (1 + \ln k)]}{(1 + k^2)} \quad (30.30)$$

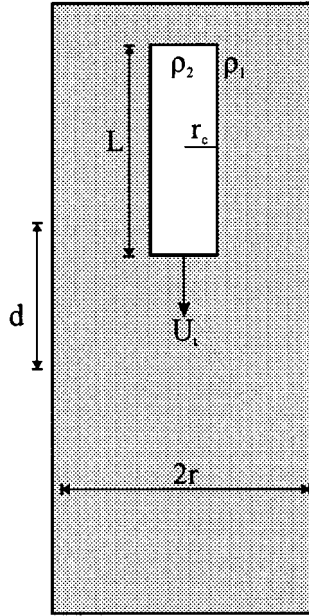


FIGURE 30.8 Schematic diagram of the falling cylinder viscometer. Using the same principle as the falling sphere, the velocity of the cylinder is obtained, which is needed to determine the shear viscosity of the fluid.

Unlike the fluid flow around a falling sphere, the fluid motion around a falling flat-ended cylinder is very complex. The effects of container ends are minimized by creating a small gap between the cylinder and the container wall. If a long cylinder (here, a cylinder is considered long if $\psi \geq 10$, where $\psi = L/r$) with a radius nearly as large as the radius of the container is used, then the effects of the walls would dominate, thereby reducing the end effects to a second-order effect. A major drawback with this approach is, however, if the cylinder and container are not concentric, the resulting inhomogeneous wall shear force would cause the downward motion of the cylinder to become eccentric. The potential for misalignment motivated the recently obtained analytical solution to the fluid flow about the cylinder ends [16]. An analytical expression for the end correction factor (ECF) was then deduced [17] and is given as:

$$\frac{1}{\text{ECF}} = 1 + \left(\frac{8k}{\pi C_w} \right) \left(\frac{G(k)}{\psi} \right) \quad (30.31)$$

where $C_w = 1.003852 - 1.961019k + 0.9570952k^2$. C_w was derived semi-empirically [17] as a disk wall correction factor. This is based on the idea that the drag force on the ends of the cylinder can be described by the drag force on a disk. Equation 30.31 is valid for $\psi \leq 30$ and agrees with the empirically derived correction [16] to within 0.6%.

With wall and end effects taken into consideration, the working formula to determine the shear viscosity of a Newtonian fluid from a falling cylinder viscometer is:

$$\eta = \frac{\left[g r_c^2 (\rho_2 - \rho_1) G(k) \right]}{\left(\frac{2U_t}{\text{ECF}} \right)} \quad (30.32)$$

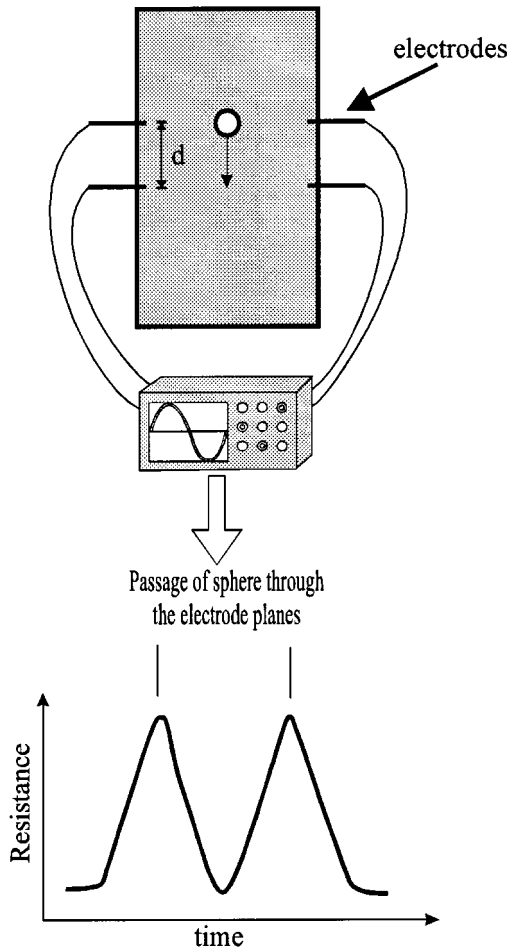


FIGURE 30.9 Diagram of one type of apparatus used to determine the viscosity of opaque liquids *in situ*. The electrical signal from the passage of the falling sphere indicates the time to traverse a known distance (d) between the two sensors.

In the past, this method was primarily used as a method to determine relative viscosities between transparent fluids. It has only been since the introduction of the ECF [16, 17] that this method could be rigorously used as an absolute viscosity method. With a properly designed container and cylinder, this method is now able to provide accurate absolute viscosities from 10^{-3} Pa·s to 10^7 Pa·s.

Falling Methods in Opaque Liquids

The falling body methods described above have been extensively applied to transparent liquids where optical (often visual) observation of the falling body is possible. For *opaque liquids*, however, falling body methods require the use of some sensing technique to determine, often *in situ*, the position of the falling body with respect to time. Techniques have varied but they all have in common the ability to detect the body as it moves past the sensor. A recent study at high pressure [18] demonstrated that the contrast in electric conductivity between a sphere and opaque liquid could be exploited to dynamically sense the moving sphere if suitably placed electrodes penetrated the container walls as shown in the schematic diagram in [Figure 30.9](#). References to other similar *in situ* techniques are given in [18].

Rising Bubble/Droplet

For many industrial processes, the rising bubble viscometer has been used as a method of comparing the relative viscosities of transparent liquids (such as varnish, lacquer, and beer) for decades. Although its use was widespread, the actual behavior of the bubble in a viscous liquid was not well understood until long after the method was introduced [19]. The rising bubble method has been thought of as a derivative of the falling sphere method; however, there are primary differences between the two. The major physical differences are (1) the density of the bubble is less than that of the surrounding liquid, and (2) the bubble itself has some unique viscosity. Each of these differences can, and do, lead to significant and extremely complex rheological problems that have yet to be fully explained. If a bubble of gas or droplet of liquid with a radius, r_b , and density, ρ' , is freely rising in some enclosing viscous liquid of density ρ , then the shear viscosity of the enclosing liquid is determined by:

$$\eta = \left(\frac{1}{\varepsilon} \right) \frac{[2gr_b^2(\rho - \rho')]}{9U_t} \quad (30.33)$$

where

$$\varepsilon = \frac{(2\eta + 3\eta')}{3(\eta + \eta')} \quad (30.34)$$

where η' is the viscosity of the bubble. It must be noted that when the value of η' is large (solid spheres), $\varepsilon = 1$, which reduces Equation 30.33 to Equation 30.25. For small values of η' (gas bubbles), ε becomes $2/3$, and the viscosity calculated by Equation 30.33 is 1.5 times greater than the viscosity calculated by Equation 30.25. It is apparent from Equation 30.33 and 30.25 that if the density of the bubble is less than the density of the enclosing liquid, and the terminal velocity of the sphere is negative, which indicates upward motion since the downward direction is positive.

During the rise, great care must be taken to avoid contamination of the bubble and its surface with impurities in the surrounding liquid. Impurities can diffuse through the surface of the bubble and combine with the fluid inside. Because the bubble has a low viscosity, the upward motion in a viscous medium induces a drag on the bubble that is responsible for generating a circulatory motion within it. This motion can efficiently distribute impurities throughout the whole of the bubble, thereby changing its viscosity and density. Impurities left on the surface of the bubble can form a "skin" that can significantly affect the rise of the bubble, as the skin layer has its own density and viscosity that are not included in Equation 30.33. These surface impurities also make a significant contribution to the inhomogeneous distribution of interfacial tension forces. A balance of these forces is crucial for the formation of a spherical bubble. The simplest method to minimize the above effects is to employ minute bubbles by introducing a specific volume of fluid (gas or liquid), with a syringe or other similar device, at the lower end of the cylindrical container. Very small bubbles behave like solid spheres, which makes interfacial tension forces and internal fluid motion negligible.

In all rising bubble viscometers, the bubble is assumed to be spherical. Experimental studies of the shapes of freely rising gas bubbles in a container of finite extent [20] have shown that (to 1% accuracy) a bubble will form and retain a spherical shape if the ratio of the radius of the bubble to the radius of the confining cylindrical container is less than 0.2. These studies have also demonstrated that the effect of the wall on the terminal velocity of a rising spherical bubble is to cause a large decrease (up to 39%) in the observed velocity compared to the velocity measured within an unbounded medium. This implies that the walls of the container influence the velocity of the rising bubble sooner than its geometry. In this method, end effects are known to be large. However, a rigorous, analytically or empirically derived

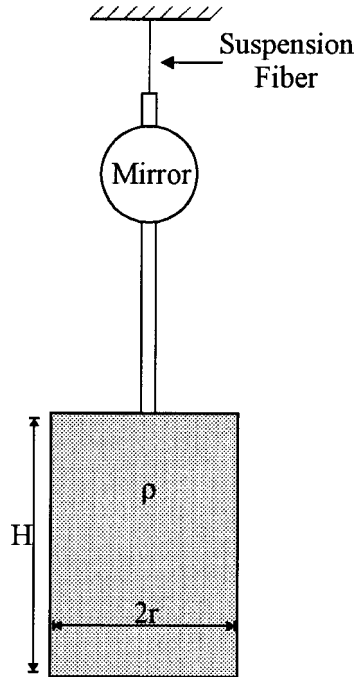


FIGURE 30.10 Schematic diagram of the oscillating cup viscometer. Measurement of the logarithmic damping of the amplitude and period of vessel oscillation are used to determine the absolute shear viscosity of the liquid.

correction factor has not yet appeared. To circumvent this, the ratio of container length to sphere diameter must be in the range of 10 to 100. As in other Stokian methods, this allows the bubble's velocity to be measured at locations that experience negligible end effects.

Considering all of the above complications, the use of minute bubbles is the best approach to ensure a viscosity measurement that is least affected by the liquid to be investigated and the container geometry.

Oscillating Method

If a liquid is contained within a vessel suspended by some torsional system that is set in oscillation about its vertical axis, then the motion of the vessel will experience a gradual damping. In an ideal situation, the damping of the motion of the vessel arises purely as a result of the *viscous coupling* of the liquid to the vessel and the viscous coupling between layers in the liquid. In any practical situation, there are also frictional losses within the system that aid in the damping effect and must be accounted for in the final analysis. From observations of the amplitudes and time periods of the resulting oscillations, a viscosity of the liquid can be calculated. A schematic diagram of the basic set-up of the method is shown in Figure 30.10. Following initial oscillatory excitation, a light source (such as a low-intensity laser) can be used to measure the amplitudes and periods of the resulting oscillations by reflection off the mirror attached to the suspension rod to give an accurate measure of the logarithmic decrement of the oscillations (δ) and the periods (T).

Various working formulae have been derived that associate the oscillatory motion of a vessel of radius r to the absolute viscosity of the liquid. The most reliable formula is the following equation for a cylindrical vessel [21]:

$$\eta = \left[\frac{I\delta}{(\pi r^3 HZ)} \right]^2 \left[\frac{1}{\pi \rho T} \right] \quad (30.35)$$

where

$$Z = \left(\frac{1+r}{4H}\right)a_0 - \frac{\left(\frac{3}{2} + \frac{4r}{\pi H}\right)}{p} + \frac{\left(\frac{3}{8} + \frac{9r}{4H}\right)a_2}{2p^2} \quad (30.36)$$

$$p = \left(\frac{\pi\rho}{\eta T}\right)^{1/2} r \quad (30.37)$$

$$a_0 = 1 - \left(\frac{\delta}{4\pi}\right) - \left(\frac{3\delta^2}{32\pi^2}\right) \quad (30.38)$$

$$a_2 = 1 + \left(\frac{\delta}{4\pi}\right) + \left(\frac{\delta^2}{32\pi^2}\right) \quad (30.39)$$

I is the mass moment of inertia of the suspended system and ρ is the density of the liquid.

A more practical expression of Equation 30.35 is obtained by introducing a number of simplifications. First, it is a reasonable assumption to consider δ to be small (on the order of 10^{-2} to 10^{-3}). This reduces a_0 and a_2 to values of 1 and -1 , respectively. Second, the effects of friction from the suspension system and the surrounding atmosphere can be experimentally determined and contained within a single variable, δ_0 . This must then be subtracted from the measured δ . A common method of obtaining δ_0 is to observe the logarithmic decrement of the system with an empty sample vessel and subtract that value from the measured value of δ . With these modifications, Equation 30.35 becomes:

$$\frac{(\delta - \delta_0)}{\rho} = \left[A \left(\frac{\eta}{\rho}\right)^{1/2} - B \left(\frac{\eta}{\rho}\right) + C \left(\frac{\eta}{\rho}\right)^{3/2} \right] \quad (30.40)$$

where

$$A = \left(\frac{\pi^{3/2}}{I}\right) \left[1 + \left(\frac{r}{4H}\right) Hr^3 T^{1/2} \right] \quad (30.41)$$

$$B = \left(\frac{\pi}{I}\right) \left[\left(\frac{3}{2}\right) + \frac{4r}{\pi H} \right] Hr^2 T \quad (30.42)$$

$$C = \left(\frac{\pi^{1/2}}{2I}\right) \left[\left(\frac{3}{8}\right) + \frac{9r}{4H} \right] Hr T^{3/2} \quad (30.43)$$

It has been noted [22] that the analytical form of Equation 30.40 needs an empirically derived, instrument-constant correction factor (ζ) in order to agree with experimentally measured values of η . The discrepancy between the analytical form and the measured value arises as a result of the above assumptions. However, these assumptions are required as there are great difficulties involved in solving

the differential equations of motion of this system. The correction factor is dependent on the materials, dimensions, and densities of each individual system, but generally lies between the values of 1.0 and 1.08. The correction factor is obtained by comparing viscosity values of calibration materials determined by an individual system (with Equation 30.35) and viscosity values obtained by another reliable method such as the capillary method.

With the above considerations taken into account, the final working Roscoe's formula for the absolute shear viscosity is:

$$\frac{(\delta - \delta_0)}{\rho} = \zeta \left[A \left(\frac{\eta}{\rho} \right)^{1/2} - B \left(\frac{\eta}{\rho} \right) + C \left(\frac{\eta}{\rho} \right)^{3/2} \right] \quad (30.44)$$

The *oscillating cup method* has been used, and is best suited for use with low values of viscosity within the range of 10^{-5} Pa s to 10^{-2} Pa·s. Its simple closed design and use at high temperatures has made this method very popular when dealing with liquid metals.

Ultrasonic Methods

Viscosity plays an important role in the absorption of energy of an *acoustic wave* traveling through a liquid. By using ultrasonic waves (10^4 Hz $< f < 10^8$ Hz), the elastic, viscoelastic, and viscous response of a liquid can be measured down to times as short as 10 ns. When the viscosity of the fluid is low, the resulting time scale for structural relaxation is shorter than the ultrasonic wave period and the fluid is probed in the relaxed state. High-viscosity fluids subjected to ultrasonic wave trains respond as a stiff fluid because structural equilibration due to the acoustic perturbation does not go to completion before the next wave cycle. Consequently, the fluid is said to be in an unrelaxed state that is characterized by dispersion (frequency-dependent wave velocity) and elastic moduli that reflect a much stiffer liquid. The frequency dependence of the viscosity relative to some reference viscosity (η_0) at low frequency, η/η_0 , and of the absorption per wavelength, $\alpha\lambda$, where α is the absorption coefficient of the liquid and λ is the wavelength of the compressional wave, for a liquid with a single relaxation time, t , is shown in [Figure 30.11](#). The maximum absorption per wavelength occurs at the *relaxation frequency* when $\omega\tau = 1$

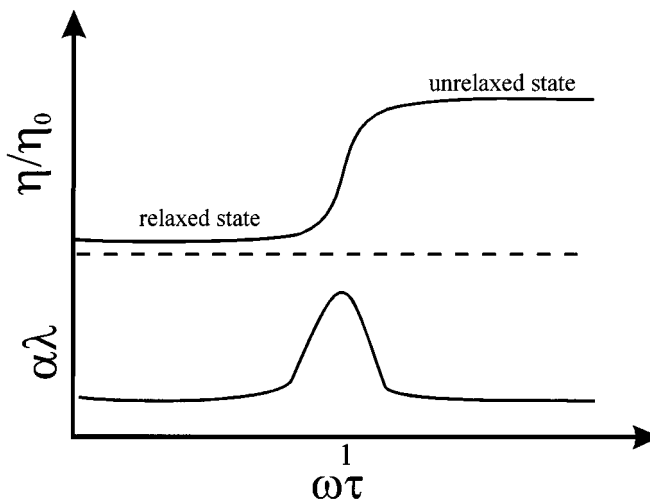


FIGURE 30.11 Effects of liquid relaxation (relaxation frequency corresponds to $\omega\tau = 1$ where $\omega = 2\pi f$) on relative viscosity (upper) and absorption per wavelength (lower) in the relaxed elastic ($\omega\tau < 1$) and unrelaxed viscoelastic ($\omega\tau > 1$) regimes.

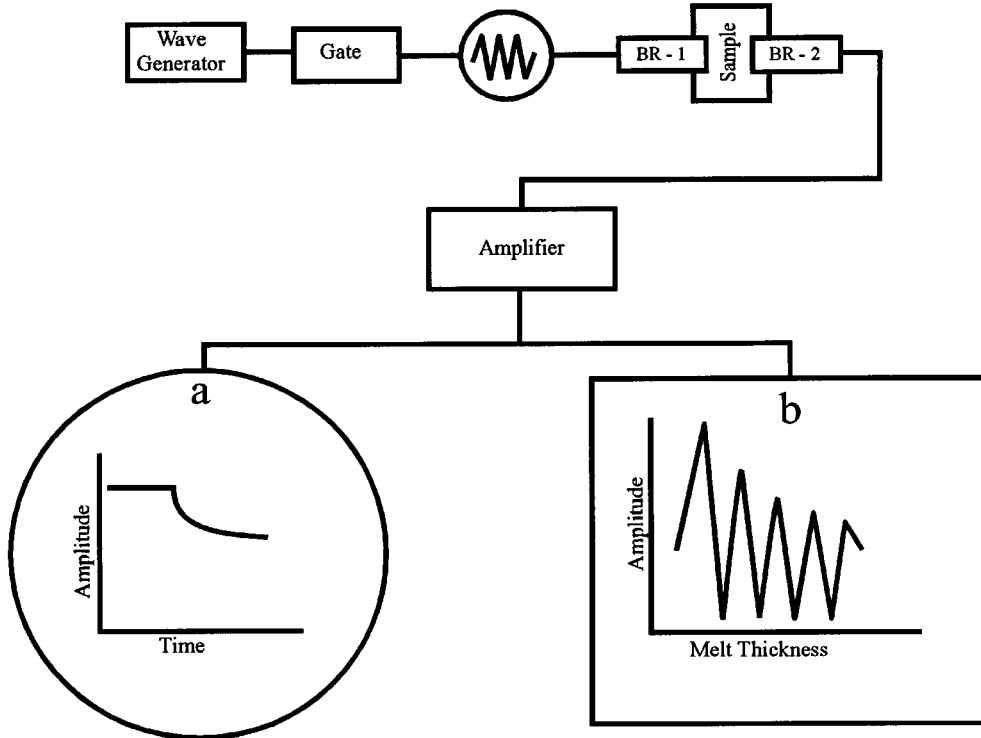


FIGURE 30.12 Schematic diagram of apparatus for liquid shear and volume viscosity determination by ultrasonic wave attenuation measurement showing the received signal amplitude through the exit buffer rod (BR-2) using (a) a fixed buffer rod (BR-2) using (a) a fixed buffer rod configuration, and (b) an interferometric technique with moveable buffer rod.

and is accompanied by a step in η/η_0 , as well as in other properties such as velocity and compressibility. Depending on the application of the measured properties, it is important to determine if the liquid is in a relaxed or unrelaxed state.

A schematic diagram of a typical apparatus for measuring viscosity by the ultrasonic method is shown in Figure 30.12. Mechanical vibrations in a piezoelectric transducer travel down one of the buffer rods (BR-1 in Figure 30.12) and into the liquid sample and are received by a similar transducer mounted on the other buffer rod, BR-2. In the fixed buffer rod configuration, once steady-state conditions have been reached, the applied signal is turned off quickly. The decay rate of the received and amplified signal, displayed on an oscilloscope on an amplitude vs. time plot as shown in Figure 30.12(a), gives a measure of α . The received amplitude decays as:

$$A = A_0 e^{-(b+\alpha c)t'} \quad (30.45)$$

where A is the received decaying amplitude, A_0 is the input amplitude, b is an apparatus constant that depends on other losses in the system such as due to the transducer, container, etc. that can be evaluated by measuring the attenuation in a standard liquid, c is the compressional wave velocity of the liquid, and t' is time. At low frequencies, the absorption coefficient is expressed in terms of volume and shear viscosity as:

$$\left(\eta_v + \frac{4\eta}{3} \right) = \frac{\alpha \rho c^3}{2\pi^2 f^2} \quad (30.46)$$

One of the earliest ultrasonic methods of measuring attenuation in liquids is based on *acoustic interferometry* [23]. Apart from the instrumentation needed to move and determine the position of one of the buffer rods accurately, the experimental apparatus is essentially the same as for the fixed buffer rod configuration [24]. The measurement, however, depends on the continuous acoustic wave interference of transmitted and reflected waves within the sample melt as one of the buffer rods is moved away from the other rod. The attenuation is characterized by the decay of the maxima amplitude as a function of melt thickness as shown on the interferogram in Figure 30.12(b). Determining α from the observed amplitude decrement involves numerical solution to a system of equations characterizing complex wave propagation [25]. The ideal conditions represented in the theory do not account for such things as wave front curvature, buffer rod end nonparallelism, surface roughness, and misalignment. These problems can be addressed in the amplitude fitting stage but they can be difficult to overcome. The interested reader is referred to [25] for further details.

Ultrasonic methods have not been and are not likely to become the mainstay of fluid viscosity determination simply because they are more technically complicated than conventional viscometry techniques. And although ultrasonic viscometry supplies additional related elastic property data, its niche in viscometry is its capability of providing volume viscosity data. Since there is no other viscometer to measure η_v , ultrasonic absorption measurements play a unique role in the study of volume viscosity.

References

1. T. A. Litovitz and C. M. Davis, Structural and shear relaxation in liquids, in W. P. Mason (ed.), *Physical Acoustics: Principles and Methods, Vol. II. Part A, Properties of Gases, Liquids and Solutions*, New York: Academic Press, 1965, 281-349.
2. Y. Bottinga and P. Richet, Silicate melts: The “anomalous” pressure dependence of the viscosity, *Geochim. Cosmochim. Acta*, 59, 2725-2731, 1995.
3. J. Ferguson and Z. Kemplowski, *Applied Fluid Rheology*, New York: Elsevier, 1991.
4. R. W. Whorlow, *Rheological Techniques*, 2nd ed., New York: Ellis Horwood, 1992.
5. K. Walters, *Rheometry*, London: Chapman and Hall, 1975.
6. J. M. Dealy, *Rheometers for Molten Plastics*, New York: Van Nostrand Reinhold, 1982.
7. J. R. Van Wazer, J. W. Lyons, K. Y. Kim, and R. E. Colwell, *Viscosity and Flow Measurement*, New York: Interscience, 1963.
8. C. W. Macosko, *Rheology: Principles, Measurements, and Applications*, New York: VCH, 1994.
9. W. A. Wakeham, A. Nagashima, and J. V. Sengers (eds.), *Measurement of the Transport Properties of Fluids*, Oxford, UK: Blackwell Scientific, 1991.
10. J. A. Himenez and M. Kostic, A novel computerized viscometer/rheometer, *Rev. Sci. Instrum.*, 65(1), 229-241, 1994.
11. DIN 53018 (Part 1 and 2), 53019, German National Standards.
12. Marks' *Standard Handbooks for Mechanical Engineers*, New York: McGraw-Hill, 1978.
13. ASTM D445-71 standard.
14. W. D. Kingery, *Viscosity in Property Measurements at High Temperatures*, New York: John Wiley & Sons, 1959.
15. H. Faxen, Die Bewegung einer Starren Kugel Langs der Achsee eines mit Zaher Flussigkeit Gefullten Rohres: *Arkiv for Matematik, Astronomi och Fysik*, 27(17), 1-28, 1923.
16. F. Gui and T. F. Irvine Jr., Theoretical and experimental study of the falling cylinder viscometer, *Int. J. Heat and Mass Transfer*, 37(1), 41-50, 1994.
17. N. A. Park and T. F. Irvine Jr., Falling cylinder viscometer end correction factor, *Rev. Sci. Instrum.*, 66(7), 3982-3984, 1995.
18. G. E. LeBlanc and R. A. Secco, High pressure stokes' viscometry: a new *in-situ* technique for sphere velocity determination, *Rev. Sci. Instrum.*, 66(10), 5015-5018, 1995.
19. R. Clift, J. R. Grace, and M. E. Weber, *Bubbles, Drops, and Particles*, San Diego: Academic Press, 1978.

20. M. Coutanceau and P. Thizon, Wall effect on the bubble behavior in highly viscous liquids, *J. Fluid Mech.*, 107, 339-373, 1981.
21. R. Roscoe, Viscosity determination by the oscillating vessel method I: theoretical considerations, *Proc. Phys. Soc.*, 72, 576-584, 1958.
22. T. Iida and R. I. L. Guthrie, *The Physical Properties of Liquid Metals*, Oxford, UK: Clarendon Press, 1988.
23. H. J. McSkimin, Ultrasonic methods for measuring the mechanical properties of liquids and solids, in W.P. Mason (ed.), *Physical Acoustics: Principles and Methods, Vol. I Part A, Properties of Gases, Liquids and Solutions*, New York: Academic Press, 1964, 271-334.
24. P. Nasch, M. H. Manghnani, and R. A. Secco, A modified ultrasonic interferometer for sound velocity measurements in molten metals and alloys, *Rev. Sci. Instrum.*, 65, 682-688, 1994.
25. K. W. Katahara, C. S. Rai, M. H. Manghnani, and J. Balogh, An interferometric technique for measuring velocity and attenuation in molten rocks, *J. Geophys. Res.*, 86, 11779-11786, 1981.

Further Information

- M. P. Ryan and J. Y. K. Blevins, *The Viscosity of Synthetic and Natural Silicate Melts and Glasses at High Temperatures and 1 Bar (10^5 Pascals) Pressure and at Higher Pressures*, U.S. Geological Survey Bulletin 1764, Denver, CO, 1987, 563, an extensive compilation of viscosity data in tabular and graphic format and the main techniques used to measure shear viscosity.
- M. E. O'Neill and F. Chorlton, *Viscous and Compressible Fluid Dynamics*, Chichester: Ellis Horwood, 1989, mathematical methods and techniques and theoretical description of flows of Newtonian incompressible and ideal compressible fluids.
- J. R. Van Wazer, J. W. Lyons, K. Y. Kim, and R. E. Colwell, *Viscosity and Flow Measurement: A Laboratory Handbook of Rheology*, New York: Interscience Publishers Div. of John Wiley & Sons, 1963, A comprehensive overview of viscometer types and simple laboratory measurements of viscosity for liquids.